Asian Journal of Chemistry; Vol. 29, No. 11 (2017), 2536-2540

ASIAN JOURNAL OF CHEMISTRY

https://doi.org/10.14233/ajchem.2017.20844

Removal Efficiency of Cu^{2+}, Zn^{2+}, Fe^{2+}, Al^{3+} and Mn^{2+} from Aqueous Solution in Presence of Bentonite Using Column Adsorption

H. CHIRIRIWA* and E.B. NAIDOO

Biosorption and Water Research Laboratory Department of Chemistry, Vaal University of Technology, Private Bag X021, Vanderbijlpark, 1911 Andries Potgieter Blvd, South Africa

*Corresponding author: Fax: +27 16 9509000; Tel: +27 16 9506742; E-mail: harrychiririwa@yahoo.com

Received: 7 June 2017; *Accepted*: 17 August 2017; *Published online*: 29 September 2017; AJC-18587

In this work, the application potentiality of bentonite for the uptake of metal ions from aqueous solution in a packed bed adsorption column was investigated. The effect of bed height at fixed influent concentration and feed flow rate was determined and the adsorption capacity of the individual metal ions was obtained at different bed height. The Langmuir and Freundlich model were used to describe adsorption isotherms for bentonite. The thermodynamics of adsorption of heavy metal ions onto bentonite was described by the standard Gibb's free energy change (ΔG°), standard enthalpy change (ΔH°) and standard entropy change (ΔS°) while the pseudo first-order and pseudo second-order kinetic model was used to describe kinetic data for the bentonite. Adsorption capacity increased with increase in bed height and from the kinetic studies, the pseudo second-order kinetic model best described the kinetic data.

Keywords: Bentonite, Column adsorption, Adsorption isotherms, Kinetic models.

INTRODUCTION

Water is one of the most important resources on earth today that is highly affected by pollution. Water pollution means that dangerous chemicals or substances have reached high levels in water and can be harmful to people and animals and render the water useless for consumption [1]. Common pollutants finding their way into the water resources include waste materials such as plastic bags, bottles, tin cans, tire dust, dissolved exhaust gasses and chemicals from various industries such as mining, leather, tanneries, metal plating, steel producers and plants using water as coolant [2]. Contamination of water with toxic metal ions Hg(II), Pb(II), Cr(III), Cr(VI), Ni(II), Co(II) Cu(II), Cd(II), Ag(I), As(V) and As(III) is becoming a severe environmental and public health problem [3-6]. However, oceans and other waters away from the coast can clean up a various amounts of pollution by moving the pollutants in different directions thereby rendering them harmless. For the well-being of the growing population it is extremely important to keep these pollutants from entering the natural water system, especially as large numbers of people living in informal settlements depends on the use of water from rivers and streams [7]. The environmental impact of mining processes is hazardous and includes acid mine drainage (AMD), erosion, formation of natural depressions, loss of maltifaraciousness and tainting of soils. Consequently, there are more than 6000 abandoned mines in South Africa (MSDOM, 2009), many of these mines produce acid mine drainage [8]. As part of our continuing interest in achieving environmental detoxification, acid mine drainage was synthesized and bentonite was applied in the removal of the heavy metals present in the acid mine drainage through column absorption experiments.

EXPERIMENTAL

Synthesis of acid mine drainage: The stock solutions of Cu^{2+}, Zn^{2+}, Fe^{2+}, Al^{2+} and Mn^{2+} were obtained by preparing 0.1 mol/L of $CuSO_4{\cdot}5H_2O$, $Zn(NO_3)_2{\cdot}6H_2O$, $Al_2(SO_4)_3{\cdot}18H_2O$, $Fe(NH_4)_2SO_4{\cdot}6H_2O$ and $MnSO_4$. These solutions were mixed together in a 1 L flask. This stock solution produced was again diluted with de-ionized water to obtain the relevant initial concentrations of 40 mg/L.

Physical measurements: Fourier transform infrared spectroscopy (Thermoscientific Nicket IS10) was used to characterize the bentonite before and after the adsorption experiments as KBr discs for the solids and all data are given in wavenumbers (cm^{-1}). Metal analysis was done using an Atomic Absorption Spectrometer (Thermo scientific ICE 3000 Series). XRF (Rigaku ZSX Primus II) was used to determine the elemental compositions of the bentonite. Particle morphology was analyzed by a Scanning Electron Microscope (SEM model Tescan Vega 3 XMU).

Packed column experiment: Continuous flow adsorption experiment was performed in a glass column having an inner gauge of 2.54 cm and depth of 40.5 cm. The bentonite was packed into the column to obtain the required bed depth. The effluent was pumped downward through the column with the aid of a peristaltic pump. All the experiments were conducted at room temperature, the effluent concentration was analyzed using AAS at regular time intervals. The amount of individual ions adsorbed at breakthrough (q) can be estimated from eqn. 1 [9].

$$q = \frac{Q_v t_b C_o}{m_c} \quad (1)$$

where Q_v is the effluent flow rate (mL/min), t_b is the breakthrough time, C_o is the influent concentration (mg/L), m_c is the mass of bentonite (g).

RESULTS AND DISCUSSION

FTIR analysis: FTIR analysis were carried out in the range of 3900-400 cm^{-1}. Bending vibrations observed at 915 cm^{-1} correspond to Al-OH-Al. The Si-O bands gave strong absorption bands in the 1100-1000 cm^{-1} region, while the bands at 520 and 468 cm^{-1} are attributed to Al-O-Si and Si-O-Si bending vibrations. The band at 3435 cm^{-1} corresponds to OH frequencies with the band at 1635 cm^{-1} representing the H-O-H bending vibration of water.

XRF analysis: Table-1 shows the XRF analysis of the bentonite. Bentonite is Na-bentonite for it has a Na/Ca ratio of 0.277. Silica is the major constituent. Adsorption of Ni, Cu and Mn resulted in the increase of the metal oxides in metal loaded bentonite accompanied by a corresponding reduction in the relative content of Na, Al and Ca oxides.

TABLE-1
XRF ANALYSIS ON BENTONITE

Component	% (m/m) bentonite	Metal loaded bentonite
Na_2O	1.4416	1.3326
MgO	1.9917	1.5483
Al_2O_3	19.6247	19.5813
SiO_2	63.7412	65.5738
CuO	0.0345	0.0151
SO_3	0.7275	1.0019
K_2O	1.1440	1.1060
CaO	2.5954	1.1699
TiO_2	0.2882	0.4473
MnO	0.0750	0.1099
Fe_2O_3	8.2587	9.4573
SrO	0.0829	0.0510
ZrO_2	0.0546	0.0633

SEM analysis: The electron diffraction spectra (EDS) confirms the presence of silicon, aluminium, calcium, iron and potassium in the bentonite. Based on SEM micrograph, bentonite seems to exhibit more slightly compact stacking morphology than the spherical flakes after adsorption as shown in Figs. 1 and 2.

Effect of bed height: The adsorption of metal ions in a fixed bed column is highly affected by the quantity of adsorbent applied. Breakthrough curves obtained for individual metal ions adsorption at bed height of 5, 10 and 15 cm and at constant flow rate and influent concentration of 1.52 mL/min and 40 mg/L are presented in Figs. 3-5. The curves tend to follow a typical "S" shape and shows that both the breakthrough and exhaustion time are functions of bed height. The breakthrough and exhaustion time for the individual metal ions took place at different time interval. It was observed that as the bed height increased from 5 to 15 cm the breakthrough and exhaustion time also increased. However, the adsorption capacity of the individual metal ions onto bentonite followed a decreasing order of Mn > Al > Fe > Cu > Zn for the three bed height

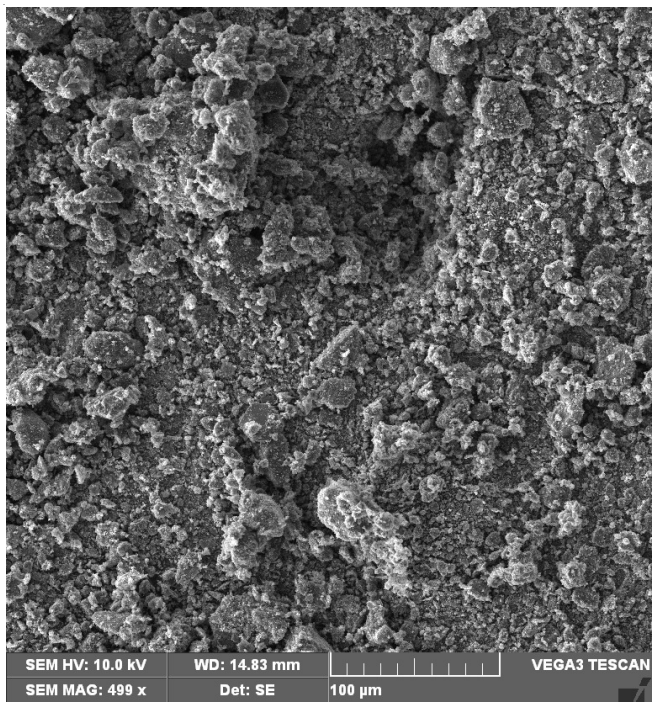

Fig. 1. Bentonite SEM micrograph before column adsorption

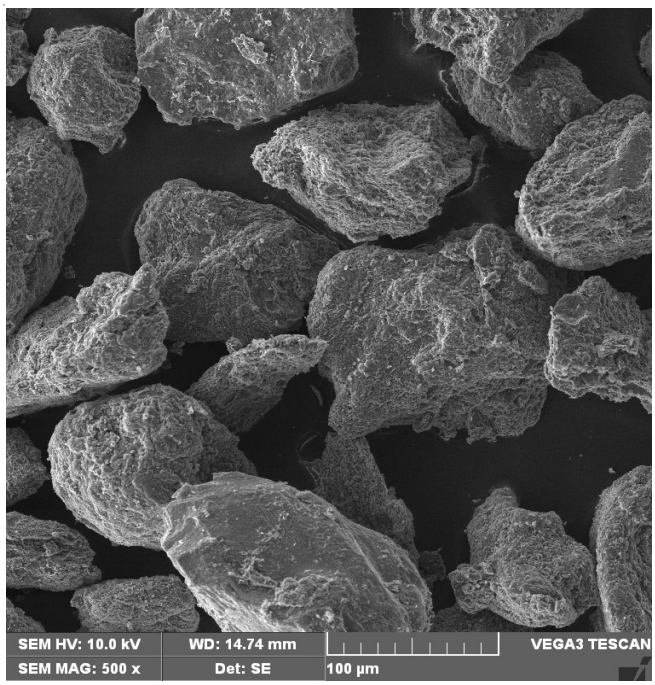

Fig. 2. Bentonite SEM micrograph after column adsorption

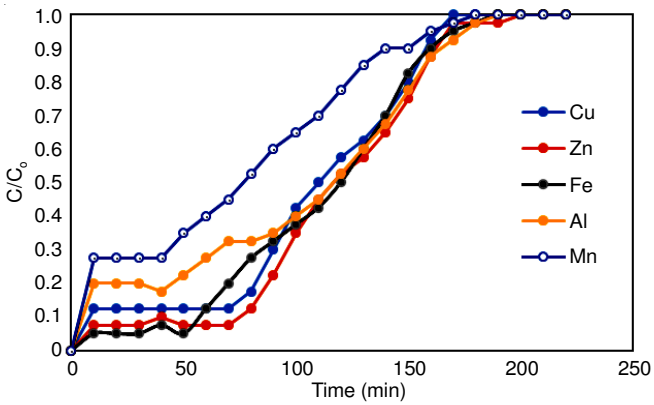

Fig. 3. Breakthrough curve for heavy metal ion adsorption onto bentonite at bed height of 5 cm, flow rate of 1.52 mL/min and influent concentration of 40 mg/L

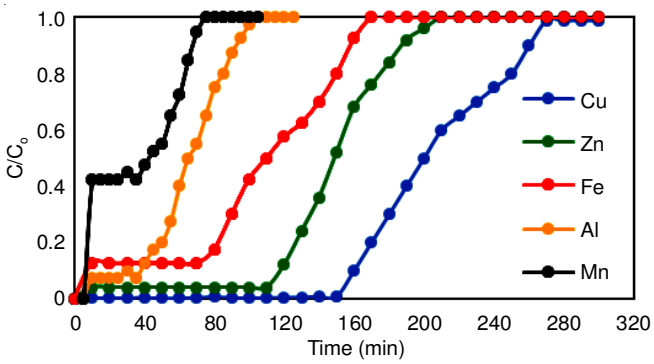

Fig. 4. Breakthrough curve for heavy metal ion adsorption onto bentonite at bed height of 10 cm, flow rate of 1.52 mL/min and influent concentration of 40 mg/L

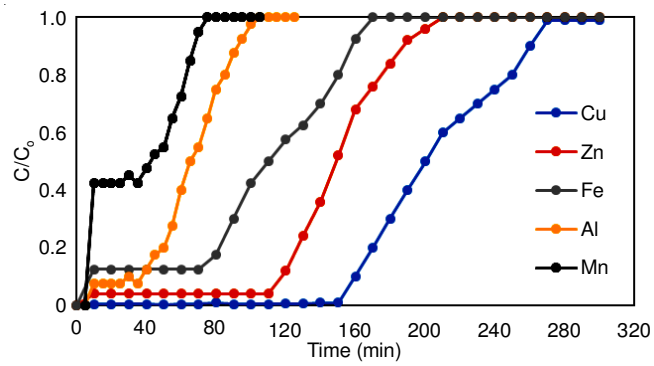

Fig. 5. Breakthrough curve for heavy metal ion adsorption onto bentonite at bed height of 15 cm, flow rate of 1.52 mL/min and influent concentration of 40 mg/L

investigated. This phenomenon can be explained in terms of ionic radius as metal ions with larger radius will tend to exhibit a lower adsorption capacity. This trend was in agreement with the order of adsorption. Consequently, the adsorption capacity of the individual metal ions increased with increase in bed height. Following the order of adsorption, at bed height of 5 cm, the adsorption capacity were 120, 115, 100, 80 and 70 mg/g for Cu, Zn, Fe, Al and Mn, respectively; at bed height of 10 cm the adsorption capacity were 133, 125, 117, 93 and 86 mg/g for Cu, Zn, Fe, Al and Mn, respectively; at bed height of 15 cm the adsorption capacity were 142, 136, 125, 103 and 94 mg/g for Cu, Zn, Fe, Al and Mn, respectively. This result is important because it suggests that for good performance of the bed, a reasonable quantity of adsorbent (increased bed height) should be considered.

Adsorption isotherm parameters: The Langmuir and Freundlich model were used to determine the appropriate isotherm for heavy metal adsorption onto bentonite. These models were described in their linear form in eqns. 2 and 3 respectively.

$$\frac{C_e}{q_e} = \frac{C_e}{Q_m} + \frac{1}{Q_m b} \quad \text{(Linear form)} \qquad (2)$$

where C_e is the equilibrium concentration (mg/L) and q_e the amount adsorbed at equilibrium (mg/g). The Langmuir constant Q_m (mg/g) represent the maximum adsorption capacity and b (l/mg) relates to the rate adsorption. Higher values of b indicate much stronger affinity of metal ion adsorption [10].

$$\log q_e = \log K_F + \frac{1}{n}\log C_e \quad \text{(Linear form)} \qquad (3)$$

K_F and n are constant representing the adsorption capacity and adsorption intensity respectively. Under normal adsorption conditions, the values of n should be in the range of 1 to 10 [11].

The parameters of the two models at different temperatures (25, 35 and 45 °C), were calculated from the slope and intercepts of C_e/q_e *versus* C_e and log q_e *versus* log C_e plots and the results are shown in Table-2.

TABLE-2
LANGMUIR AND FREUNDLICH ISOTHERM PARAMETERS AT DIFFERENT TEMPERATURES

Metal ions	Isotherm model	Parameters	25 °C	35 °C	45 °C
Copper	Langmuir	Q_m (mg/g)	30.3	47.6	52.6
		b (l/mg)	0.011	0.014	0.014
		R^2	0.971	0.942	0.943
	Freundlich	1/n	0.539	0.544	0.579
		K_F (mg/g)	1.19	2.06	3.44
		R^2	0.969	0.932	0.950
Zinc	Langmuir	Q_m (mg/g)	83.3	90.9	100
		b (l/mg)	0.070	0.20	0.32
		R^2	0.988	0.956	0.957
	Freundlich	1/n	0.396	0.429	0.510
		K_F (mg/g)	12.27	17.70	19.63
		R^2	0.985	0.935	0.953
Iron	Langmuir	Q_m (mg/g)	55.4	65.4	86.8
		b	0.031	0.34	0.21
		R^2	0.987	0.997	0.998
	Freundlich	1/n	0.22	0.26	0.28
		K_F (mg/g)	15.23	22.12	24.54
		R^2	0.879	0.898	0.943
Aluminum	Langmuir	Q_m (mg/g)	60.55	70.38	88.98
		b	0.01	0.05	0.09
		R^2	0.995	0.999	0.965
	Freundlich	1/n	0.32	0.43	0.49
		K_F	21.22	25.21	27.65
		R^2	0.914	0.922	0.942
Manganese	Langmuir	Q_m (mg/g)	70.33	83.76	98.45
		b	0.03	0.07	0.04
		R^2	0.999	0.999	0.987
	Freundlich	1/n	0.65	0.75	0.87
		K_F (mg/g)	18.65	22.54	27.43
		R^2	0.873	0.879	0.911

The closer R^2 is to 1 the best the model fit. The R^2 values of the Langmuir model for the metal ions investigated were all equal and greater than 0.942 and this is in contrast to the R^2

values obtained from the Freundlich model (equal and greater than 0.873) and hence the Langmuir model best describe the adsorption isotherm of bentonite. The Langmuir model however supports the existence of monolayer coverage on the adsorption site of bentonite.

Thermodynamic parameters: The plot of ln K against 1/T for bentonite is shown in Fig. 6. Table-3 gives the values of the parameters for thermodynamic studies. The free energy change (ΔG°) obtained during the absorption reaction at temperatures of 25, 35 and 45 °C were all negative and this indicates that the adsorption of heavy metals onto bentonite is spontaneous and favourable. A similar finding was reported by Zawani *et al*. [12]. The positive value of ΔH° indicates that the adsorption process is endothermic in nature. This finding is in agreement to the result presented by Liu *et al*. [11]. The positive value of ΔS° indicates the increased randomness at the solid-solution interface during the adsorption of heavy metal ions onto bentonite [11].

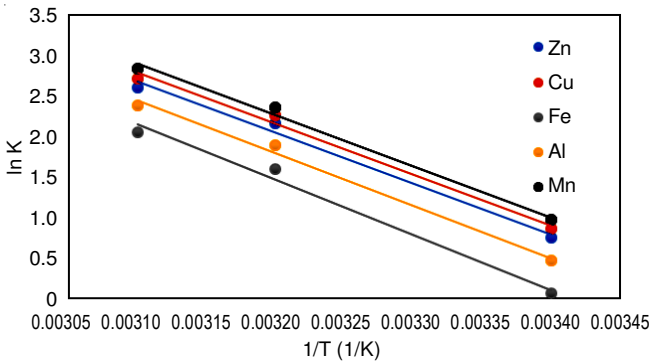

Fig. 6. Thermodynamic plot of ln K against 1/T for bentonite adsorption onto heavy metal ions

TABLE-3
THERMODYNAMIC PARAMETERS FOR THE ADSORPTION OF HEAVY METAL IONS ONTO BENTONITE AT AN INITIAL CONCENTRATION OF 200 mg/L

Metal	Temp. (K)	ΔG° (kJ/mo)	ΔH° (kJ/mol)	ΔS° (kJ/mol K)	R^2
Copper	298	-1.86	+52.67	+0.19	0.990
	308	-5.53			
	318	-6.90			
Zinc	298	-1.43	+48.78	+0.32	0.987
	308	-4.21			
	318	-7.54			
Iron	298	-2.22	+47.12	+0.11	0.996
	308	-4.11			
	318	-6.79			
Aluminium	298	-1.11	+45.89	+0.52	0.985
	308	-3.44			
	318	-6.39			
Manganese	298	-1.55	+44.67	+0.51	0.975
	308	-4.34			
	318	-5.25			

Kinetic parameters: The kinetics of adsorption is used to investigate the time course of metal ion adsorption onto bentonite. It is also important to determine whether the behaviour of metal uptake onto bentonite can be explained by a predictive model. The pseudo-first order and pseudo-second order model (eqns. 4 and 5) was used to fit the kinetic data.

$$\Delta G^\circ = -RT \ln K \quad (4)$$

The equilibrium constant 'K' as defined mathematically by Liu *et al*. [11]

$$\frac{dq_t}{et} = K_2(q_e - q_t)^2 \quad (5)$$

were K_2 is the rate constant for a pseudo-second order model and the definitions of q_e and q_t remain the same.

Studies have shown that the pseudo-second order kinetic model gives a better fit for adsorption data [13]. Table-2 gives the values of the parameters for a pseudo-first and second order kinetic model and it was observed that the correlation coefficients for the straight plot of t/q_t against t from the pseudo-second order rate law are equal and greater than 0.994, in contrast to the correlation coefficient (≥ 0.896) of the pseudo-first order kinetic model obtained from the linear plot of log $(q_e - q_t)$ against t. Figs. 7 and 8 elucidate the kinetic plot for pseudo first and second order model respectively. This linear correlation coefficient method of determination of best fit model suggests that the adsorption of metal ions onto bentonite is a pseudo-second order reaction model.

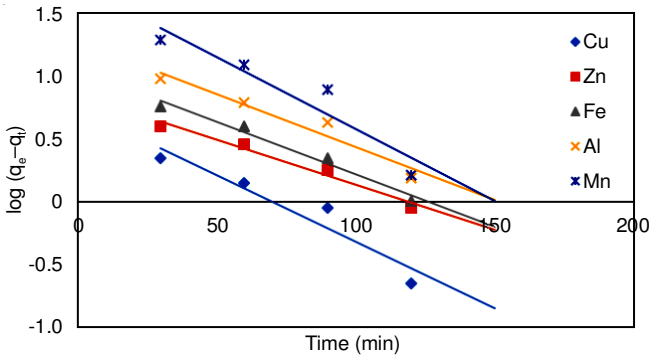

Fig. 7. Pseudo first order kinetic model plot

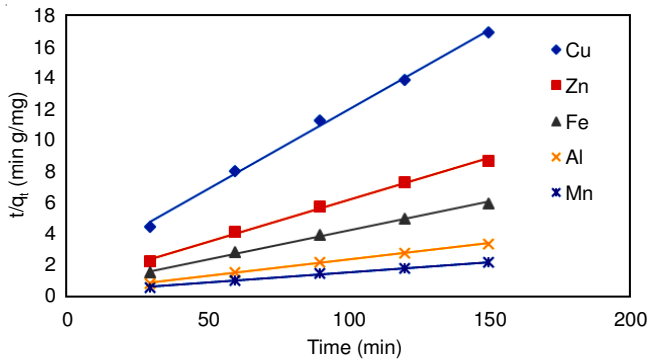

Fig. 8. Pseudo second order kinetic model plot

To further investigate kinetic data the chi-square test (χ^2) of statistical analysis was applied. Table-4 showed the values of χ^2 for the pseudo first-order kinetic model and pseudo second-order kinetic model were similar. For example at a concentration of 40 mg/L the χ^2 for pseudo first-order and pseudo second-order kinetic model were 0.03 and 0.11 respectively. However, there was a large difference for q_e values obtained by calculating from pseudo first-order kinetic model and experimental values. For example, at 40 mg/L the value of $q_{e(Cal)}$ from pseudo first-order kinetic model is 5.57 mg/g and the value of $q_{e(Exp)}$ is 8.89

TABLE-4
KINETIC PARAMETERS FOR THE ADSORPTION OF HEAVY METALS ONTO BENTONITE

Metal ion	First-order kinetic model					Second-order kinetic model			
	K_1 (min)	$q_{e(Cal)}$ (mg/g)	χ^2	R^2	$q_{e(Exp)}$ (mg/g)	K_2 (g/mg min)	$q_{e(Cal)}$ (mg/g)	R^2	χ^2
Cu	0.020	5.57	0.03	0.913	8.89	5.93×10^{-3}	9.90	0.997	0.11
Zn	0.016	7.13	0.07	0.973	17.31	3.34×10^{-3}	18.87	0.995	0.19
Fe	0.020	11.25	0.03	0.973	25.34	2.31×10^{-3}	27.78	0.997	0.30
Al	0.020	19.10	0.05	0.943	44.44	1.38×10^{-3}	50.00	0.997	0.43
Mn	0.030	52.60	0.10	0.896	67.78	6.31×10^{-4}	76.90	0.996	0.91

mg/g. In case of the pseudo second-order model, q_{eCal} values agreed very well with the experimental data, such that from pseudo second-order model, the q_{eCal} value for copper is 9.90 mg/g, which is very close to q_{eExp} having a value of 8.89 mg/g. This suggests that the adsorption of metal ions onto bentonite is a pseudo-second order reaction model and this model is based on the assumption that the rate limiting step may be chemical adsorption or chemisorption involving valence forces through exchange of electrons between adsorbate (metal ions) and adsorbent (bentonite), provides best correlation of data [14,15].

Conclusion

It was considered in this study that bentonite has the ability of binding very strongly with harmful heavy metal ions. This property along side with its availability and low cost distinguishes the adsorbent from a number of adsorbents described in literature by various authors. In considering the adsorption of heavy metals it is necessary to consider the most important parameter, which is the bed height. The adsorption capacity of the individual metal ions onto bentonite followed a decreasing order of Mn > Al > Fe > Cu > Zn for the three bed heights investigated. This phenomenon was attributed in terms of ionic radius as metal ions with larger radius will tend to exhibit a lower adsorption capacity. This trend was in agreement with the order of adsorption. Consequently, the models applied in describing the experimental data were adequate.

ACKNOWLEDGEMENTS

This work was supported by CHIETA (Strategic Contract-0170). E. Igberase is gratefully acknowledged for carrying out the experimental work

REFERENCES

1. J. Berger, M. Reist, J.M. Mayer, O. Felt, N.A. Peppas and R. Gurny, *Eur. J. Pharm. Biopharm.*, **57**, 19 (2004); https://doi.org/10.1016/S0939-6411(03)00161-9.
2. T. Falayi and F. Ntuli, *J. Ind. Eng. Chem.*, **20**, 1285 (2014); https://doi.org/10.1016/j.jiec.2013.07.007.
3. M. Ahmaruzzaman, *Adv. Colloid Interface Sci.*, **166**, 36 (2011); https://doi.org/10.1016/j.cis.2011.04.005.
4. C. Williams, D. Aderhold and G.J. Edyvean, *Water Res.*, **32**, 216 (1998); https://doi.org/10.1016/S0043-1354(97)00179-6.
5. K. Kadirvelu, K. Thamaraiselvi and C. Namasivayam, *Bioresour. Technol.*, **76**, 63 (2001); https://doi.org/10.1016/S0960-8524(00)00072-9.
6. L. Muza, D. Dube, A. Ochieng and H. Chirariwa, *Iran. J. Sci. Technol. Trans. A: Sci.*, 1 (2016); https://doi.org/10.1007/s40995-016-0102-z.
7. A. Luptakova, S. Ubaldini, E. Macingova, P. Fornari and V. Giuliano, *Process Biochem.*, **47**, 1633 (2012); https://doi.org/10.1016/j.procbio.2012.02.025.
8. The National Strategy for the Management of Derelict and Ownerless Mines (MSDOM) in South Africa, Department of Mineral Resources, vol. 2 (2009).
9. V.C. Taty-Costodes, H. Fauduet, C. Porte and A. Delacroix, *J. Hazard. Mater.*, **105**, 121 (2003); https://doi.org/10.1016/j.jhazmat.2003.07.009.
10. M.R. Kasaai, *Carbohydr. Polym.*, **79**, 801 (2010); https://doi.org/10.1016/j.carbpol.2009.10.051.
11. D. Liu, D. Sun and Y. Li, *J. Separ. Sci. Technol.*, **46**, 321 (2011); https://doi.org/10.1080/01496395.2010.504201.
12. Z. Zawani, C.A. Luqman and S.Y.C. Thomas, *Eur. J. Scient. Res.*, **37**, 63 (2009).
13. Y. Sag and Y. Aktay, *J. Biochem. Eng.*, **12**, 143 (2002); https://doi.org/10.1016/S1369-703X(02)00068-2.
14. Y.S. Ho and G. Mckay, *Water Res.*, **33**, 578 (1999); https://doi.org/10.1016/S0043-1354(98)00207-3.
15. Y.S. Ho and G. Mckay, *Chem. Eng. J.*, **70**, 115 (1998); https://doi.org/10.1016/S0923-0467(98)00076-1.